Adsorption (2009) 15: 287–299
DOI 10.1007/s10450-009-9176-7

Controlling adsorption and release of drug and small molecules by organic functionalization of mesoporous materials

Tewodros Asefa · Amy N. Otuonye · Gang Wang · Elizabeth A. Blair · Rajyalakshmi Vathyam · Kelley Denton

Published online: 17 April 2009

Abstract A series of mesoporous nanosphere materials that are functionalized with various terminal and bridging organic groups were synthesized. They have improved adsorption capacity and different release properties for drug and small molecules. The materials contained terminal vinyl, 3-mercaptopropyl, 3-aminopropyl, and secondary amine functional groups and bridging ethane, ethene, and benzene groups within their mesopore channel walls. The samples containing mercaptopropyl and vinyl groups showed greater adsorption capacity and better controlled release behavior for rhodamine 6G molecules. On the other hand, mesoporous matrices containing amine functional groups showed higher adsorption capacity and better release properties for ibuprofen molecules. Further studies revealed that the bridging organic groups in the mesopore channel walls also improved the adsorption capacity and release properties of the materials compared to the corresponding samples containing no bridging organic groups. Such improved adsorption and controlled release properties of molecules by simple changes of functional groups on mesoporous materials are important for the development of nanomaterial drug delivery vehicles and for controlled release of drugs over long time periods at specific targeted sites in the body. By judicious choice of organic groups and by systematic design and synthetic approaches, nanoporous materials having different adsorption capacity and release properties for many other drug molecules can also be achieved.

T. Asefa (✉) · A.N. Otuonye · G. Wang · E.A. Blair · R. Vathyam · K. Denton
Department of Chemistry, Syracuse University, Syracuse, New York 13244, USA
e-mail: tasefa@syr.edu

Keywords Multifunctional mesoporous materials · Drug delivery · Periodic mesoporous organosilica · Controlled drug release · Organofunctional mesoporous materials

1 Introduction

The design and synthesis of novel nanostructured materials containing high surface area, well-ordered nanostructures and "smart" functional groups have been drawing considerable attention because such materials have potential for catalysis, drug-delivery, biosensing, and for microfluidic and bioseparation applications (Whitesides 2005; Kim et al. 2006; Law et al. 2005; Thomas and Raja 2001; Corriu et al. 2004). By synthesizing functionalized nanostructured platforms that have high surface area, nanometer structures, pore sizes as well as tunable surface properties, it is also possible to control the adsorption and release properties of drug molecules and to use the resulting materials as drug carriers (Giri et al. 2007; Horcajada et al. 2006; Vallet-Regi 2006; Zeng et al. 2006; Yang et al. 2007a, 2007b). When the functional groups include specific bioactive groups such as antibodies and peptide nucleic acids (PNAs), the functionalized nanomaterials will also allow efficient treatments of various diseases possibly by getting therapy to places in the body that are otherwise inaccessible. This in turn can prevent the body's normal defenses from getting in the way before treatments reach targets and reduce the chance that healthy tissue will be damaged (Gadre and Gouma 2006). Designing a controlled drug release system by functionalization of nanomaterials will also help to minimize adverse reactions which lead to many unwanted side effects (Mal et al. 2003). With current drug administration methods, the drug might pass through various physiologic obstacles as it travels to the desired site thus decreasing the

amount of drug that actually reaches the required site. The decrease in efficacy for many drugs is caused by an inability to deliver the drug molecules to specific cells or tissues. By improving the adsorption capacity, controlled drug release, and specificity of nanomaterials via organic functionalization, it is possible to improve their site specific delivery and increase the drug's efficacy (Wu et al. 2004).

Since the discovery of mesoporous materials in 1992 (Yanagisawa et al. 1990; Kresge et al. 1992; Beck et al. 1992; Inagaki et al. 1993), research efforts for the synthesis of these materials with various types of functional groups and composition for a number of applications have exploded (Sayari and Hamoudi 2001; Fryxell et al. 1999; Hicks et al. 2006; Zapilk et al. 2007). Functionalized mesoporous materials are of interest to biological and medical researchers because their properties such as high surface areas (typically 1,000 m^2/g) and their nanometer range pore sizes (2–30 nm pore diameter) allow for high adsorption of bioactive and drug molecules and for producing suitable drug carrying vehicles for biological and medical applications (Vallet-Regi et al. 2007; Lai et al. 2003; Tang et al. 2006). Another beneficial property of mesoporous materials is their tunable nanometer pore sizes that enable the immobilization of different size molecules (Moller and Bein 1998). For instance, the large pore channels of SBA-15 mesoporous materials can accommodate larger bioactive molecules (Song et al. 2005) while smaller mesopores of MCM-41 materials can hold smaller bioactive molecules (Zhu et al. 2005). Furthermore, the surfaces of mesoporous silica materials can be modified by the addition of different organic groups, either during the synthesis or after the synthesis of the materials (Stein et al. 2000; Asefa et al. 1999; Holland et al. 1999; Inagaki et al. 1999). Functionalizing the mesopore walls with organic groups allows tuning the surface properties of the materials and enables controlling the adsorption and release of drug and bioactive molecules, thus judiciously altering the drug delivery properties of the materials (Balas et al. 2006; Tang et al. 2006; Doadrio et al. 2006; Horcajada et al. 2006; Vallet-Regi 2006; Zeng et al. 2006; Yang et al. 2007a, 2007b; Yang et al. 2008; Huang et al. 2008).

The organic functionalization of mesoporous materials also enables systematic control of the materials' pore selectivity for entrance and release of molecules (Zapilk et al. 2007; Anan et al. 2008). Generally, pore selectivity of mesoporous materials can be dictated by the pore shape and size and/or the covalent interactions between the functional groups on the surfaces of mesopores and the guest molecules. By partially replacing the silica precursor (or alkoxysilanes) with organosilanes, it is possible to introduce organic groups into the mesoporous materials and to tune their pore diameters (Kruk et al. 2002; Asefa et al. 1999; Holland et al. 1999; Inagaki et al. 1999). It also results in an increase in non-covalent interactions between guest molecules and the material's surface because of the hydrophobicity or hydrophilicity of the organic groups (Anan et al. 2008; Walcarius et al. 2003). This further improves the immobilization of hydrophobic or hydrophilic drugs and enzymes into the pores the mesoporous material. The possibility of inclusion of secondary functional groups such as antibodies or fluorophores on the external surfaces of the mesoporous materials further enables targeting specific biological sites or bioimaging tissues (Radu et al. 2004). Such multifunctional properties of nanoporous and mesoporous materials as a result of organic functionalization allow for great potential for controlled drug delivery at targeted cells in the body by mesoporous materials (Gu et al. 2007).

Here we report on the synthesis of various multifunctional nanomaterials containing different monofunctional and multifunctional groups that have different adsorption capacity and release properties for drug and small molecules. The functional groups included terminal vinyl, mercaptopropyl and aminopropyl groups and bridging ethane, ethylene, and phenylene groups. The samples containing mercaptopropyl and vinyl groups showed greater adsorption capacity and better controlled drug release property for rhodamine 6G molecules. On the other hand, mesoporous matrices containing amine functional groups showed higher adsorption capacity and better release properties for ibuprofen molecules. Further studies revealed that bridging organic groups also improved the adsorption capacity of the materials for rhodamine 6G compared to the corresponding samples containing no bridging organic groups. Improving adsorption and release properties by such simple change of the functional groups on mesoporous nanomaterials is important for the development of nanomaterials for controlled release of drugs. By judicious choice of organic groups and by systematic design and synthesis, nanoporous materials having different adsorption capacity and release properties for other molecules can also be produced. Rhodamine 6G and ibuprofen were chosen because of their different hydrophobic or hydrophilic properties and because they allow the investigation of interaction of molecules with functionalized mesoporous materials. Furthermore they are easy to probe and were previously used for similar studies to monitor drug adsorption and release properties of mesoporous materials (Qu et al. 2006; Dong et al. 2007; Patel et al. 2008; Suh et al. 2008; Yang et al. 2007a, 2007b).

2 Experimental

Materials and reagents. Cetyltrimethylammonium bromide (CTAB), tetraethoxysilane (TEOS), 3-aminoproyltriethoxysilane (APTS), bis(triethoxysilylpropyl)amine (BTSPA), vinyltriethoxysilane (VTS), 1,2-bis(triethoxysilyl)ethylene (BTE), 1,4-bis(trethoxysilyl)phenylene (BTP),

rhodamine 6G (R6G), and sodium salt of ibuprofen were all obtained from Sigma-Aldrich and they were used as received without further purification. 3-Mercaptopropyltrimethoxysilane (MPTS) and 1,2-bis(triethoxysilyl)ethane (BTSE) were obtained from Gelest, Inc. Anhydrous toluene and isopropanol were purchased from Pharmco-AAPER.

Synthesis of a series of monofunctional mesoporous materials containing terminal organic groups by co-condensation. Monofunctional mesoporous materials were synthesized by co-assembly of TEOS with four different terminal organosilanes, namely APTS, MPTS, BTSPA, and VTS. Typically, 33.4 mL distilled water and 15 mL ammonium hydroxide were mixed and stirred for 1 min. Then 0.84 g CTAB was added and the solution was stirred for 5 min. A mixture of TEOS (15.4 mmol) and a terminal organosilane (3.8 mmol) of MPTS (or VTS, APTS, or AAPTS) was added. The mixture was stirred at room temperature for 2 h and stored in an oven at 80 °C for 2 days. Then it was allowed to cool for 5 min and filtered over Whatman-1 filter paper. The solid was washed thoroughly five times with copious amount of water and dried under ambient conditions. The surfactant template was extracted by stirring 2 g of the functionalized mesostructured material in a solution of 50 mL methanol and 10 mL HCl for 5 h at 50 °C. The solution was filtered over a Whatman-1 filter paper and the solid was washed with copious amount of water three times and then with 20 mL ethanol. The solid sample was allowed to dry under ambient conditions. The resulting samples were labeled as Co-VTS, Co-MPTS, Co-APTS, and Co-BTSPA for the samples synthesized from VTS, MPTS, APTS, and BTSPA, respectively.

Synthesis of a series of multifunctional mesoporous materials containing terminal and bridging organic groups by co-condensation. Multifunctional mesoporous samples were synthesized by co-assembling bridging organosilane (BTSE, BTE, or BTP) with TEOS and a terminal organosilane MPTS. Typically, 33.4 mL distilled water and 15 mL ammonium hydroxide were mixed and stirred for 1 min. Then 0.84 g CTAB was added and the solution was stirred for 5 min. To this solution, a mixture of 7.7 mmol TEOS, 3.8 mmol of BTSE, and 3.8 mmol of a terminal organosilane MPTS was added. The solution was stirred at room temperature for 2 h and stored in an oven at 80 °C for 2 days. The sample was then removed from the oven and allowed to cool for 5 min. The sample was filtered and the solid was washed, and dried under ambient conditions. The surfactant template was extracted by stirring 2 g of the functionalized mesostructured material in a solution of 50 mL methanol and 10 mL HCl for 5 h at 50 °C. The solution was filtered over a Whatman-1 filter paper and the solid was washed with copious amount of water three times and then with 20 mL ethanol. The solid sample was allowed to dry under ambient conditions. The samples from BTE and BTP were also synthesized by following the same procedures.

Synthesis of functionalized mesoporous materials by post-grafting terminal organic groups. First mesoporous silica (MCM-41) was synthesized as reported previously. Typically, 33.4 mL of distilled water and 15 mL ammonium hydroxide were mixed and stirred for 1 min. Then 0.84 g of CTAB was added and the solution was stirred for 5 min. To this solution was added 4 g of TEOS and stirring of the solution was continued moderately at room temperature for 30 min. The solution was aged in an oven at 80 °C for 2 days. Then the sample was removed from the oven and allowed to cool for 5 min. The solution was filtered over Whatman-1 filter paper and the solid was washed five times using 40 mL of distilled water. The solid was let to dry under ambient conditions. This resulted in mesostructured silica sample. The surfactant template from the sample was then extracted to produce mesoporous silica by stirring 2 g of the mesostructured silica in a solution containing 50 mL of methanol and 4 mL of HCl for 5 h at 50 °C. The solution was filtered over Whatman-1 filter paper. The solid was washed thoroughly with distilled water and dried under ambient conditions. This resulted in mesoporous silica (MCM-41) sample.

To synthesize the functionalized materials by post-grafting, 400 mg of extracted MCM-41 and 250 mL of ethanol were placed in a round bottom flask. Then, 2.2 mmol of the terminal organosilane (for example, APTS) in 100 mL toluene was added and the solution was stirred moderately at 80 °C for 6 h. The solution was then filtered over Whatman-1 filter paper. The solid was washed with 500 mL of ethanol and then let to dry. This post-grafting of MPTS, VTS, and BTSPA was conducted by following the same procedures (Scheme 1). These samples were labeled as Graftiing-APTS, Grafting-MPTS, Grafting-VTS, and Grafting-BTSPA.

Adsorption of rhodamine 6G. A solution of rhodamine 6G (R6G) with a concentration of 0.6 μM was prepared in distilled water at room temperature. Then, 0.1 g of each functionalized mesostructured material and 10 mL of R6G solution were placed in a falcon tube and stirred for 10 min. The samples were centrifuged for 10 min. The supernatant was analyzed by the UV-Vis spectroscopy. The prominent absorption maximum peak for R6G was monitored at ∼526 nm. After analysis by UV-Vis spectroscopy, the supernatant was returned to the falcon tubes and the solution was stirred further. After another 10 minutes, the solution was centrifuged and the supernatant was tested again by UV-Vis spectroscopy. This procedure was repeated until the sample had stopped adsorbing more dye. Similar adsorption experiments were also performed for all the other samples by following the same procedures.

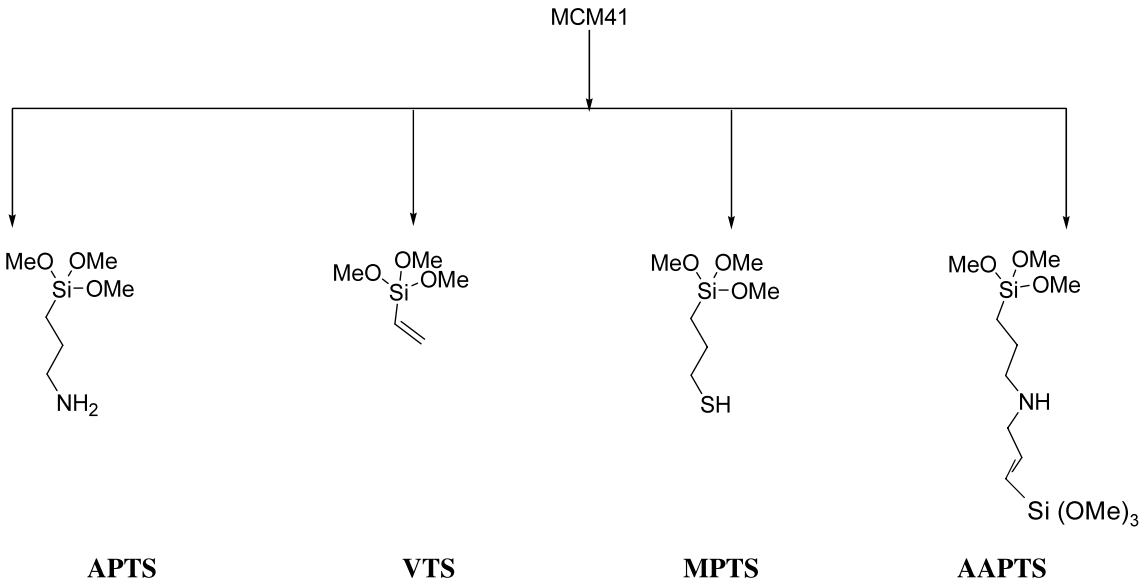

Scheme 1 Scheme of functionalizing by post-grafting of extracted MCM-41

Adsorption of ibuprofen. First, ibuprofen was prepared from sodium salt of ibuprofen by acidifying 10 g of sodium salt of ibuprofen in 160 mL of 1 M HCl solution for 1 h at room temperature. The solution was then kept in an ice bath to let the ibuprofen crystallize and precipitate. The solution was filtered and the ibuprofen crystals were washed with 50 mL water and let to dry under ambient conditions. A stock solution of 100 mL ibuprofen solution with a concentration of 40 mg/mL was prepared in anhydrous ethanol. Then, 0.1 g of the functionalized mesoporous sample and 5 mL of the ibuprofen solution were mixed. After 5 min, the sample was centrifuged, and the supernatant was taken and analyzed with UV-Vis spectroscopy by monitoring the prominent absorption peak of ibuprofen at 264 nm. The supernatant was returned to the vial, and after additional 5 min, it was centrifuged. This step was repeated until the sample had stopped adsorbing ibuprofen. Similar experiments were performed for all samples.

Release of rhodamine 6G. To study the release properties of rhodamine 6G (R6G), 0.1 g of the functionalized mesoporous samples and 100 mL of water at pH = 7.00 were mixed and stirred. The solution was centrifuged at intervals of time (typically 10 min) and 1 mL of the release medium or supernatant was removed for analysis by UV-Vis spectroscopy at the given time intervals. The prominent absorption maximum of R6G at 526 nm was monitored. The extract was returned into the solution, let to stir for an additional 5 min time, centrifuged again, and the absorption maximum at 526 nm was monitored.

Release of ibuprofen. For the studies of ibuprofen release, a simulated body fluid (SBF) solution was used. The SBF solution was prepared as reported previously (Kokubo et al. 1990). Typically, 0.1 g functionalized mesoporous sample and 100 mL SBF at pH 7.4 at 37 °C were mixed and stirred. Then 1 mL of the release medium was removed for analysis every 1 or 2 h intervals and replaced with the same volume of fresh preheated SBF solution. The extract was analyzed using UV-Vis spectroscopy and by monitoring the peak at 264 nm.

Instrumentations. The powder X-ray diffraction (XRD) was measured using a Scintag powder diffractometer. The solid-state ^{13}C (75.5 MHz) and ^{29}Si (59.6 MHz) nuclear magnetic resonance (NMR) spectra were acquired on a Bruker AVANCE 300 spectrometer. For ^{13}C CP-MAS NMR experiments, we employed 7.0 kHz spin rate, 5 s recycle delay, 1 ms contact time, $\pi/2$ pulse width of 5.2 μs, and 1,000–3,000 scans using TPPM 1H decoupling. For the ^{29}Si CP-MAS NMR experiments, we used 7.0 kHz spin rate, 10 s recycle delay, 10 ms contact time, $\pi/2$ pulse width of 5.6 μs, and 256–1,024 scans using TPPM ^{1}H decoupling. The thermogravimetric analysis (TGA) was carried out with a Q-500 Quantachrome Instrument (TA-Instruments). The BET gas adsorptions were measured with Micromeritics Tristar-3000 BET instrument. The UV-Vis absorption spectra were measured using a Lambda 950 UV-Vis-NIR spectrophotometer (Perkin-Elmer). The transmission electron microscopy (TEM) images were taken by using a FEI Tecnai T-12 transmission electron microscope.

Scheme 2 Chemical structures of different terminal and bridging organosilanes and TEOS used for the synthesis of multifunctional mesoporous materials

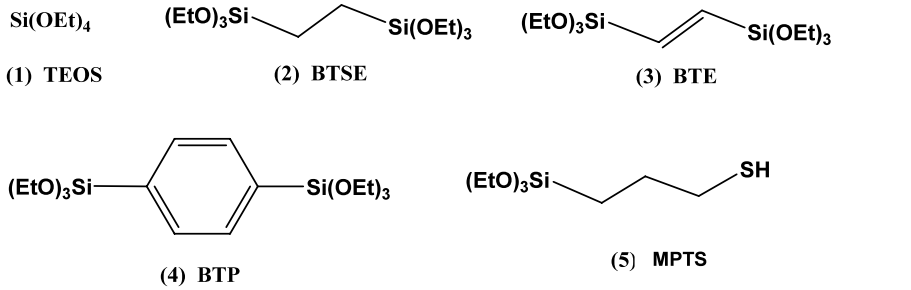

3 Results and discussion

3.1 Synthesis and characterization of functionalized mesoporous materials

The synthesis of a series of functionalized mesoporous materials was performed via a "bottom-up" templating technique involving supramolecular surfactant self-assembly of organosilanes and alkoxysilanes (Cheng et al. 1995; Lim et al. 1997; Margolese et al. 2000) or by post-grafting the organosilanes onto the surfaces of pre-made mesoporous silica (Sharma and Asefa 2007; Sharma et al. 2008). The supramolecular self-assembly of mesostructured silica materials requires alkoxysilanes and surfactant in aqueous solution (Huo et al. 1996). Surfactants such as cetyltrimethylammonium bromide (CTAB) in aqueous solution form micellar structures above their critical micellar concentration (CMC). The hydrolysis and condensation of alkoxysilanes or the sol gel process will undergo around these micellar aggregates and produce ordered mesostructured solid-state materials. The surfactant–alkoxysilane solution is typically aged in oven at 80 °C for 48 h in order to facilitate polymerization of silicates and to help the formation of more robust mesostructured material (Yanagisawa et al. 1990; Kresge et al. 1992; Beck et al. 1992; Inagaki et al. 1993; Asefa et al. 1999). Upon extraction of the surfactant templates from the mesostructured material, a highly porous functionalized mesoporous silica containing high surface area, tunable nanometer pores and high pore volume will result.

The use of terminal or bridging organosilanes (Scheme 2) during post-grafting or co-condensation synthesis of mesoporous materials produces surface organic groups that will help to tune the surface properties of the materials into hydrophobic or hydrophilic. For instance, by post-grafting APTS on mesoporous silica, we produced mesoporous materials containing surface primary amine ($-NH_2$) groups. Similarly, the post-grafting of BTSPA produced mesoporous materials containing secondary amine (–NH–) groups. The post-grafting of MPTS onto the mesoporous silica resulted in organothiol (–SH) groups on the walls of the material. Similarly, the addition of VTS introduced vinyl (–CH = CH_2) groups on the surface of the mesoporous nanomaterials. While the amine groups made the mesoporous material hydrophilic, the thiol and vinyl groups made the materials hydrophobic. Similarly, the co-condensation bridging organosilanes BTSE, BTE, and BTP with TEOS and MPTS resulted in bifunctional mesoporous materials containing bridging and terminal organic functional groups. The functionalized mesoporous materials we synthesized either by post-grafting or co-condensation method contained terminal vinyl, mercaptopropyl, and secondary amine groups and bridging ethane, ethene, and phenylene groups. Their structures and composition were then characterized and their adsorption and release properties for rhodamine 6G and ibuprofen were investigated.

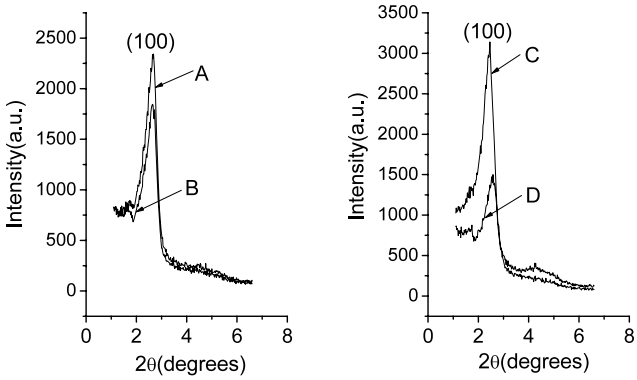

Fig. 1 (**I**) Powder X-ray diffraction (XRD) patterns of functionalized mesoporous samples synthesized by co-condensation of organosilanes (*A*) MPTS and (*B*) VTS. The corresponding XRD patterns after R6G adsorption are shown in (*C*) and (*D*), respectively

The structures of the mesoporous materials were characterized by powder X-ray diffraction (XRD) (Fig. 1). The XRD of the samples showed a (100) peak in the low 2-theta region, which is characteristic of the presence of ordered mesostructures in the materials. The unit cell values for representative samples were calculated from *d*-spacing on XRD and are given in Table 1. The degree of order of the mesostructures in the samples synthesized by co-condensation was found to be less than that of the samples synthesized by post-grafting. This is not unexpected, as the co-condensation of alkoxysilane with terminal organosilane

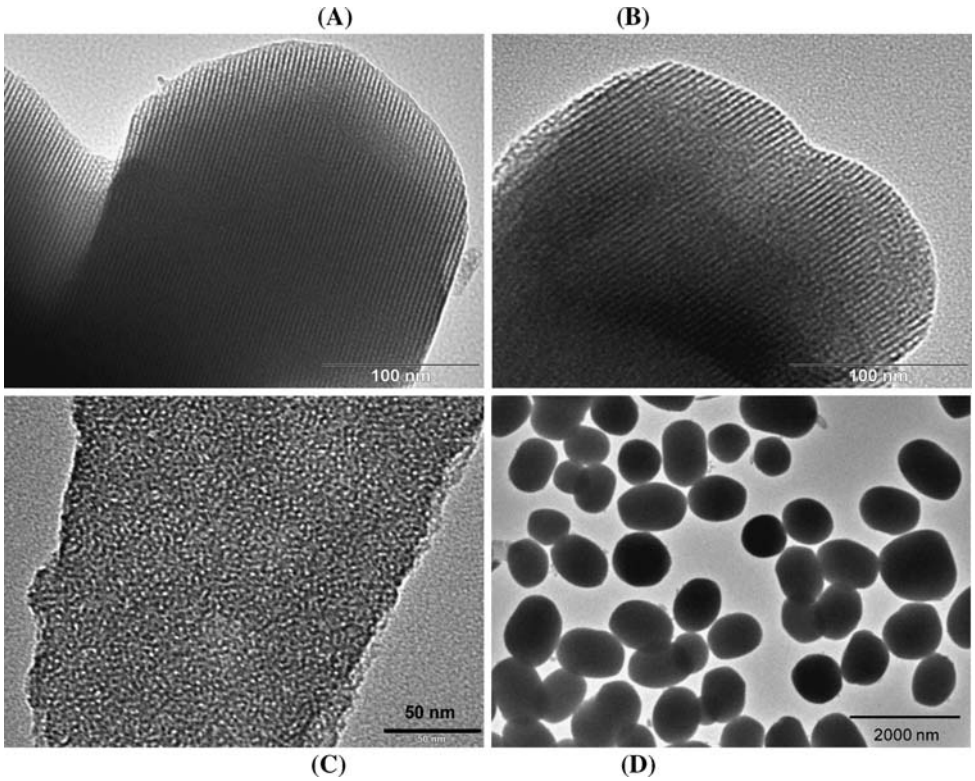

Fig. 2 TEM images of (**A**) MCM-41, (**B**) vinyl-functionalized sample by post-grafting, and (**C**) vinyl-functionalized sample by co-condensation. (**D**) A low resolution TEM image showing particle morphologies and sizes of vinyl-functionalized sample by post-grafting

Table 1 Structural information of mesoporous silica and aminofunctionalized mesoporous silica prepared by post-grafting the mesoporous silica with aminoorganosilanes in toluene

Samples	Organosilanes	Unit cell (Å)[a]	Surface area
Samples synthesized by co-condensation			
MPTS	MPTS, TEOS	44.6	543
VTS	VTS, TEOS	44.2	655
APTS	APTS, TEOS	48.8	189
BTSPA	BTSPA, TEOS	55.4	238
Samples synthesized by post-grafting in toluene			
MPTS	MPTS + MCM-41	44.1	755
VTS	VTS + MCM-41	44.0	704
APTS	APTS + MCM-41	44.3	532
BTSPA	BTSPA + MCM-41	42.4	515

[a]Unit cell of the mesostructured sample calculated from the sample's d-spacing value, which was obtained from its X-ray diffraction (XRD) pattern (Unit Cell, $a_o = 2d_{100}/3^{1/2}$ for hexagonal P_{6mm} mesostructures)

often results in mesoporous material with rather less ordered mesostructures (Kruk et al. 2002).

The mesoporous structures in the materials were further confirmed by transmission electron microscopy (Fig. 2). The TEM images showed that the materials had spherical and oval shaped morphologies with ordered or worm-hole like mesoporous structures in them (Fig. 2). In particular, the samples that were synthesized by post-grafting showed hexagonally ordered mesostructures while those synthesized by co-condensation exhibited less ordered structures and worm-hole like stuctures.

Nitrogen adsorption isotherms for some representative samples are given in Fig. 3. The isotherms are type IV, which are indicative of the presence of mesoporous structures in the samples. The capillary condensation steps of the isotherms of the materials synthesized by post-grafting were sharper and are indicative of the presence of more ordered mesoporous structures compared to those synthesized by co-condensation. Furthermore, the samples synthesized by co-condensation from VTS and MPTS showed a more steep capillary condensation steps than the corresponding samples synthesized from APTS and BTSPA. The Brunauer-Emmett-Teller (BET) surface areas of the materials were found to be to be 515–755 m^2/g for the post-grafted samples and 189–655 m^2/g for the materials synthesized by co-condensation. The BJH average pore size of the materials ranged between 2.6–3.0 nm in all the samples.

Solid-state NMR spectra confirmed that the functionalized mesoporous materials contained the desired functional groups that were added. For instance, the ^{13}C spectrum for the monofunctional sample synthesized from BTSPA and TEOS and the ^{29}Si CPMAS NMR spectrum for the bifunctional sample synthesized from BTSPA, MPTS and TEOS were given on Fig. 4. The ^{13}C CPMAS NMR spectrum shows peaks between ~10–45 ppm and at 50 ppm corre-

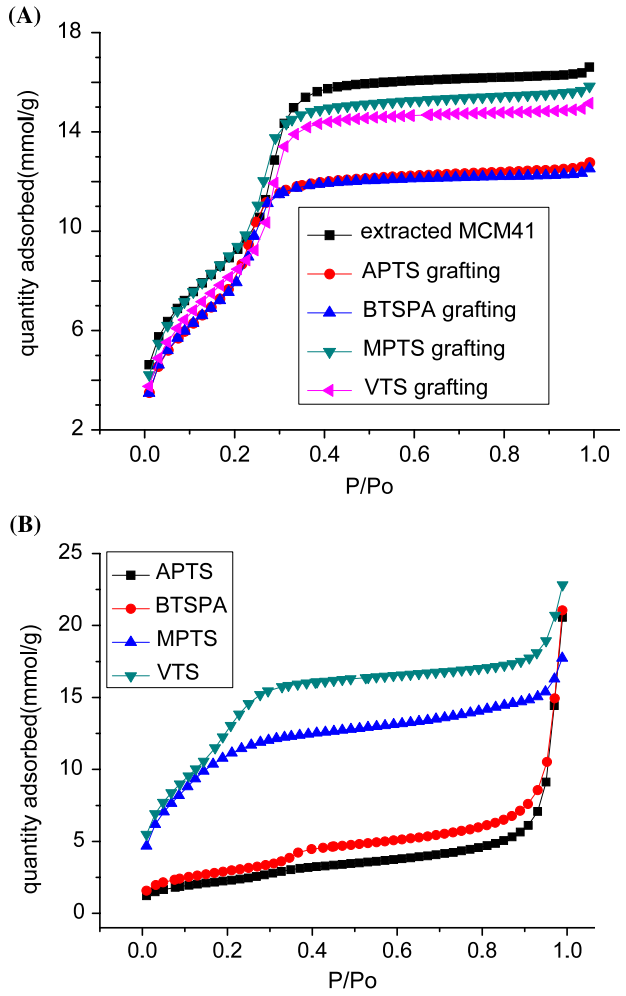

Fig. 3 (**A**) N_2 gas adsorption isotherms of functionalized mesoporous samples synthesized by (**A**) post-grafting and (**B**) co-condensation

Table 2 Weight loss between 100–500 °C and mmol/organic groups/g sample for the functionalized mesoporous samples synthesized by co-condensation

Sample	wt. % of organic groups	mmol organic groups/g of material
APTS	6.5%	112 mmol/g
BTSPA	6.0%	61 mmol/g
MPTS	14.0%	181 mmol/g
VTS	4.5%	166 mmol/g

sponding to the carbon atoms of the aminopropyl groups of BTSPA. The ^{29}Si CP-MAS NMR spectrum (Fig. 4B) also confirmed the presence of the organic in the material. The spectrum shows T^2 and T^3 peaks in the range of ∼−40 to −63 ppm, which correspond to various silicon atoms attached to aminopropyl groups (or SiRO(OH) and $SiRO_{1.5}$, respectively) as well as Q^3 and Q^4 peaks in the range of ∼−80 to −110 ppm, which correspond to the silicon atoms attached to four oxygen atoms (or $SiO_{1.5}(OH)$ and SiO_2).

Thermogravimetric traces also showed in a more general way that the organic functional groups were present in the materials (Table 2). A weight loss from below 100 °C was observed in all the samples, which was an indication of the presence of physisorbed water. Weight losses between ∼200–500 °C were also observed from the functionalized samples, which were mainly due to the decomposition of organic groups from the samples or were an indication of the presence of these groups in the materials. Further slight losses beyond 500 °C were also observed from all the materials, which was typically due to further loss of water molecules by condensation of residual surface silanol groups in the materials. Careful calculations based on the TGA data revealed that the amount of grafted organic groups in the mesoporous materials were ∼112, 61, 181, and 166 mmol/g for samples grafted with APTS, BTSPA, MPTS, and VTS, respectively. This indicated that the trend in the density of organic grafted groups decreased in the order of MPTS > VTS > APTS > BTSPA.

3.2 Adsorption and release of rhodamine 6G and ibuprofen

The adsorption of rhodamine 6G (R6G) by the different functionalized samples was then investigated. This was performed by stirring the samples with aqueous R6G solution and measuring the absorbance of the supernatant solutions after centrifugation (Fig. 5 and Table 3). R6G was chosen as a model drug molecule because it can easily be monitored by UV-Vis absorption spectroscopy (Dong et al. 2007; Patel et al. 2008; Suh et al. 2008). The UV-Vis absorption spectra of the supernatant after stirring the same mass of the four samples synthesized by co-condensation with the same concentration and volume of R6G solution for 10 min still showed absorption peaks corresponding to R6G, in case of the solutions from APTS and BTSPA but not in the solutions from MPTS and VTS (Fig. 5A). This indicated that the samples that were prepared from MPTS and VTS completely adsorbed R6G from the solution while the samples that were prepared from APTS and BTSPA did not. The differences in the adsorption properties of the samples can also be clearly seen based on the colors of the solid samples after re-suspension in water (Fig. 5B). As can be observed in Fig. 5B, the samples from MPTS and VTS appeared deep pink colored indicating that they adsorbed the most R6G, followed by those samples from BTSPA and APTS samples. By using the Beer-Lambert's formula, the concentration, moles and mass of R6G adsorbed by some representative samples were also quantitatively determined (Table 3). The materials that were synthesized by post-grafting also showed similar results as the samples that were synthesized by co-condensation (Fig. 5C). The samples post-grafted with MPTS adsorbed the most R6G, followed by samples functionalized with VTS, then APTS and BTSPA.

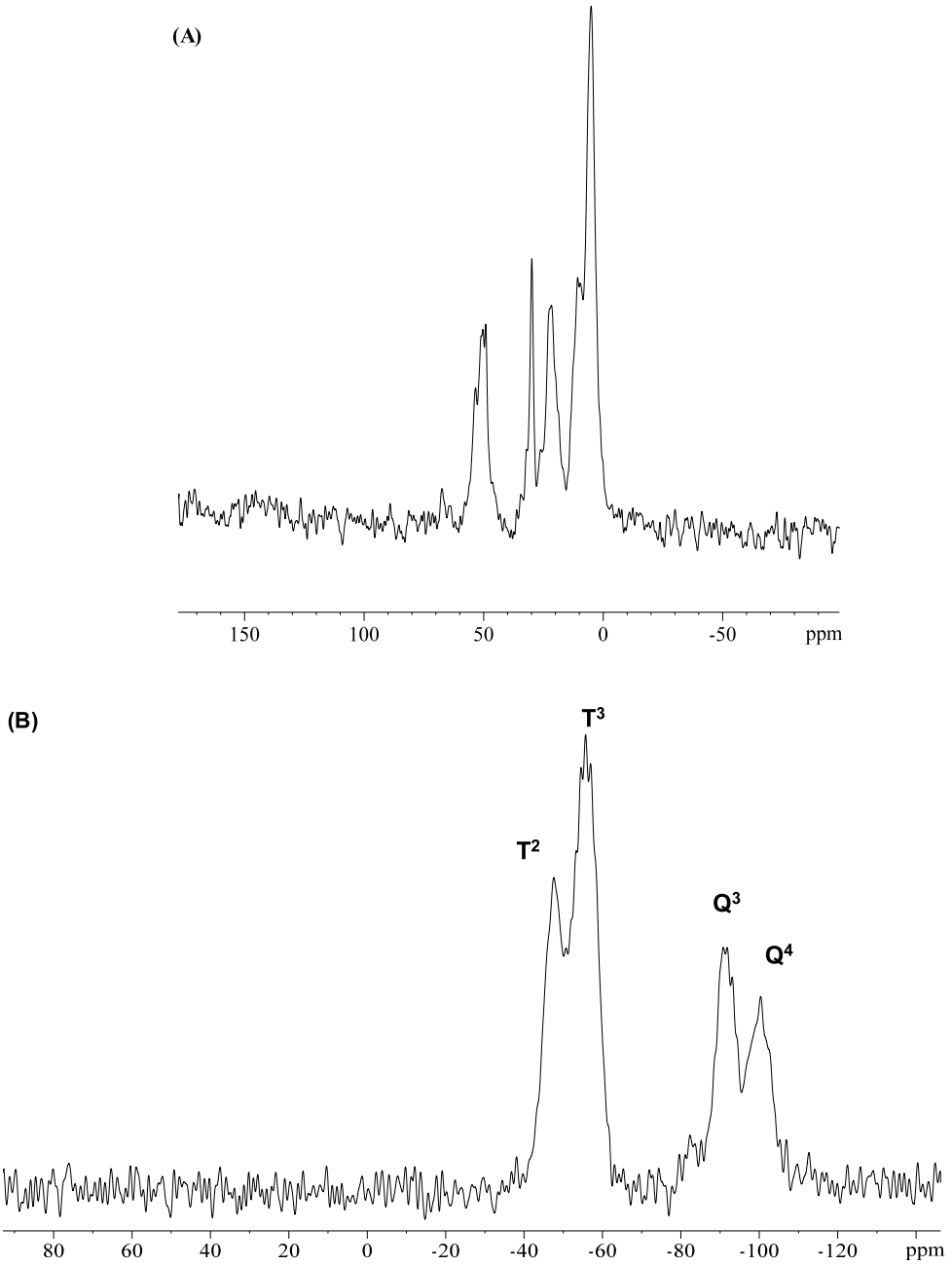

Fig. 4 (**A**) ^{13}C CP-MAS spectrum of bifunctional mesoporous sample synthesized by co-condensation of BTSPA and TEOS and (**B**) ^{29}Si CP-MAS solid-state NMR spectrum of multifunctional mesoporous sample synthesized by co-condensation of BTSE, MPTS and TEOS

Table 3 Adsorption capacity of rhodamine 6G of different samples synthesized by co-condensation and post-grafting

Sample	Adsorption capacity (μmol/g of mesoporous material)
Co-MPTS	292
Grafting-MPTS	146
Co-VTS	84
Grafting-VTS	67

The fact that the samples that were synthesized from APTS and BTSPA adsorbed less R6G was probably caused by the weaker interaction between the amine functionalized surface and R6G. Alternatively, the strong adsorption of R6G by the samples functionalized with MPTS and VTS was due to the stronger interaction between the hydrophobic mercaptopropyl and vinyl groups and the hydrophobic parts of R6G molecules (Scheme 3). The results of this experiment show that functional groups play an important role in the adsorption of R6G and therefore, functionalization can greatly influence the adsorption of substances into mesoporous material.

Release studies of rhodamine 6G from the functionalized materials that were synthesized by co-condensation and

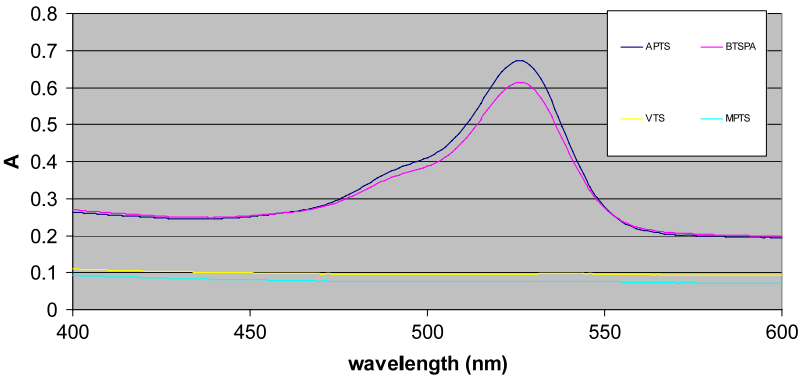

(A)

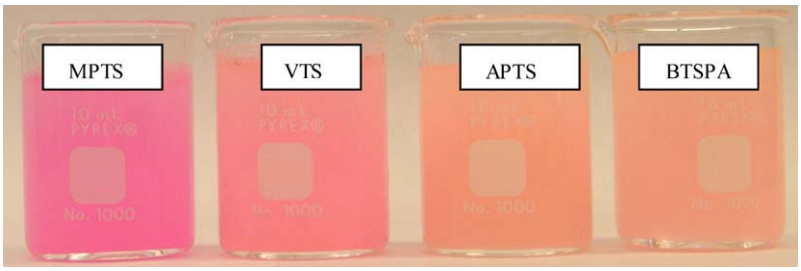

(B)

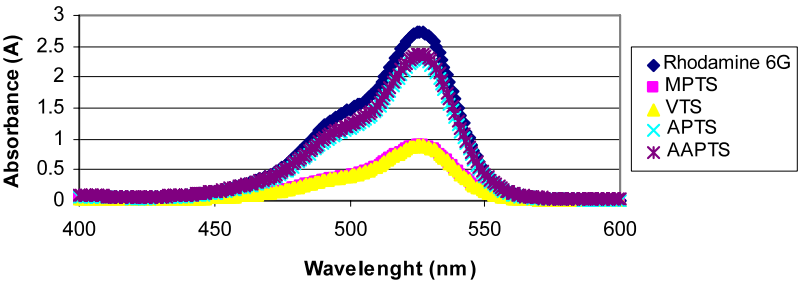

(C)

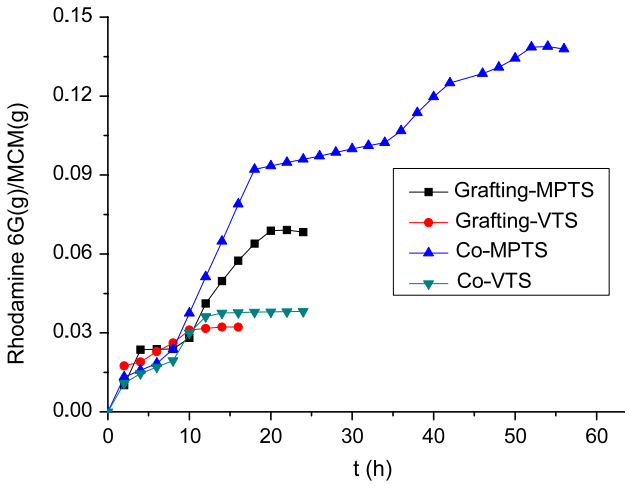

(D)

Fig. 5 Adsorption properties of rhodamine 6G by various mesoporous materials. (**A**) UV-Vis absorption spectra of R6G in the supernatant 20 minutes after adsorption of a solution of R6G with different functionalized mesoporous materials synthesized via co-condensation. (**B**) Digital images showing colors of the functionalized mesoporous silica samples synthesized by co-condensation that were re-suspended after R6G dye adsorption. A bright color was observed for the MPTS functionalized sample indicating that it has adsorbed more R6G compared to the other samples. (**C**) UV-Vis absorption spectra of R6G in the supernatant 20 minutes after adsorption of a solution of R6G with different functionalized materials that were synthesized via post-grafting. (**D**) Comparative adsorption profile of different selected samples that were synthesized by co-condensation and post-grafting

Scheme 3 Chemical structures of rhodamine 6G and ibuprofen molecules

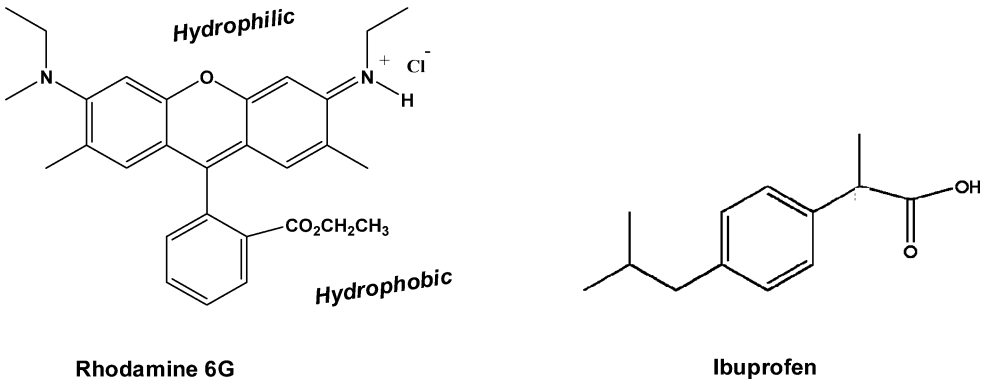

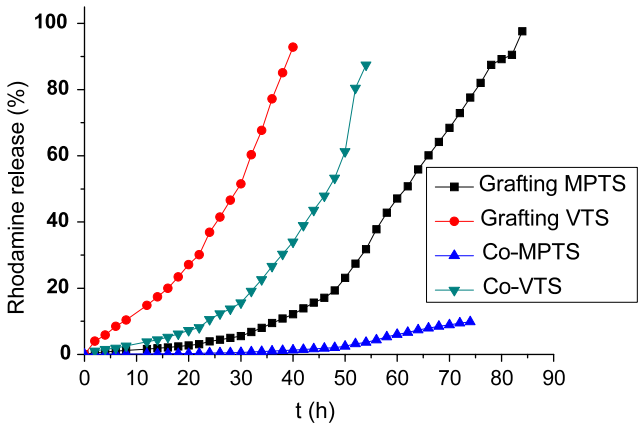

Fig. 6 Comparative studies showing graphs of percent of R6G released for selected samples synthesized by co-condensation and by post-grafting MPTS and VTS

post-grafting were then conducted. The samples functionalized with APTS and BTSPA by co-condensation released very little R6G compared to the corresponding samples functionalized with MPTS and VTS (Fig. 6). Because the latter two samples adsorbed the most R6G, they were obviously capable of releasing the most dye. The release of R6G was faster in the first few minutes but slowed down later on (Fig. 6A). Nevertheless the release of the R6G from MPTS and VTS samples has lasted for many hours in both cases, with only slight differences between the two samples. Similarly, for the samples synthesized by post-grafting, the order of R6G release was decreasing in the order of samples functionalized with VTS > MPTS > APTS > BTSPA. The release rate also followed the same trend, i.e., the sample functionalized with VTS showed more release than the sample functionalized with MPTS. Furthermore, the samples synthesized by post-grafting exhibited faster release rate than the corresponding samples synthesized by co-condensation. Mathematical calculation based on the Beer-Lambert equation was performed to find the concentration and mass of rhodamine 6G released from each sample. The results indicated that the sample functionalized with VTS released more rhodamine 6G than the other samples. Based on these results, it can be concluded that the sample functionalized with VTS was the best material for use in adsorption and release of rhodamine 6G.

The properties of the functionalized mesoporous materials were also tested for adsorption and release of a real drug, ibuprofen (Fig. 7). The functionalized samples adsorbed ibuprofen differently compared to R6G because the structure of ibuprofen and its interaction with the functional groups of the materials was different from that of R6G. For samples synthesized by co-condensation, the sample functionalized with APTS adsorbed the most ibuprofen followed by those functionalized with VTS, BTSPA and finally MPTS (Fig. 7). This trend was also true for the series of samples synthesized by post-grafting. These results indicate that the trend in the degree of adsorption of the materials for ibuprofen was a reverse of what was obtained for R6G. The stronger adsorption of ibuprofen by the samples functionalized with APTS might be because of the favorable interaction of the acidic groups of ibuprofen with the amine groups in the mesoporous samples. The adsorption of ibuprofen by the hydrophobic mesoporous samples functionalized with VTS could be due to the favorable hydrophobic interaction between the hydrophobic aromatic groups of ibuprofen and the hydrophobic surface of the mesoporous material containing vinyl groups.

The studies of ibuprofen release by the different samples were carried out in a simulated body fluid (SBF) (Kokubo et al. 1990) of pH of 7.40 at 37 °C. SBF solution has similar composition as what is in our body and therefore, many drug release experiments in SBF solution are commonly demonstrated. In this in-vitro ibuprofen release studies, the samples synthesized by co-condensation from VTS, MPTS and APTS were obtained to release more than ∼30% of their adsorbed ibuprofen in the first 5 h. The BTSPA sample, however, was unique because it did not begin to release for about 18 h but then it began to release at a high rate. Furthermore, the samples functionalized with VTS and APTS samples continued to release ibuprofen at a slightly higher rate while the sample functionalized with MPTS released the drug at a much slower rate. This is consistent with

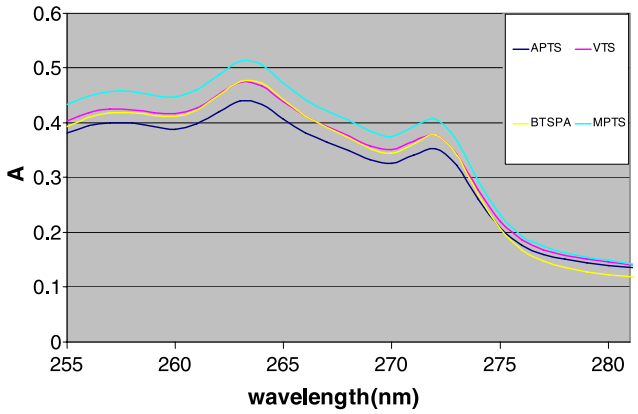

(A)

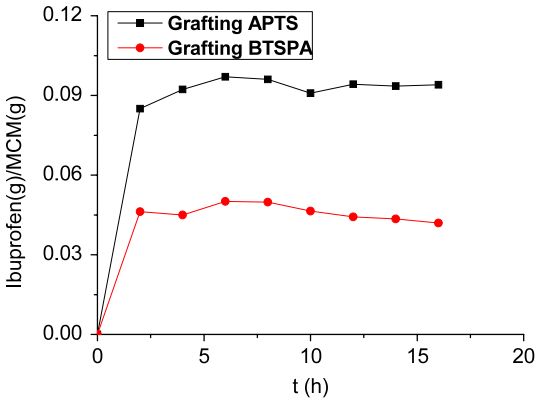

(B)

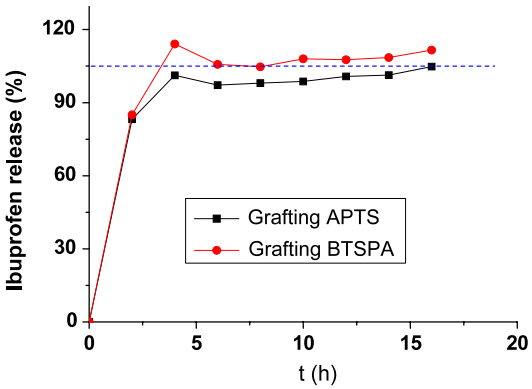

(C)

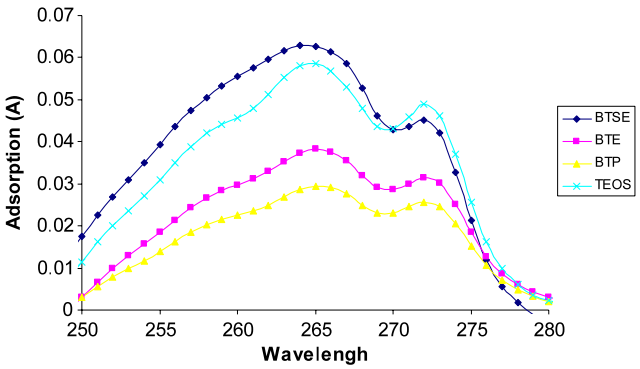

(D)

Fig. 7 Adsorption and release properties of ibuprofen by various functionalized mesoporous materials. (**A**) UV-Vis absorption spectra of ibuprofen in the supernatant after stirring with different functionalized mesoporous materials synthesized via co-condensation. (**B**) Comparative adsorption profile of ibuprofen of different selected functionalized mesoporous materials that were synthesized via post-grafting. (**C**) Comparative % release of ibuprofen of selected materials that were synthesized via post-grafting. (**D**) UV-Vis absorption spectra of total ibuprofen released in the solution 2 h after stirring a solution of ibuprofen with various functionalized mesoporous materials containing bridging ethane, ethylene, and phenylene groups as well as MCM-41

the results reported by Muñoz et al. (2003). On the other hand the BTSPA sample synthesized by grafting showed quick release of ibuprofen compared to all the other samples. Upon comparing the APTS functionalized samples by co-condensation and grafting, we found that the sample synthesized by co-condensation released the ibuprofen more quickly than that synthesized by grafting. The release of ibuprofen by the samples grafted with MPTS and VTS were very low because these samples adsorbed the molecule weakly. Interestingly, the bifunctional materials containing bridging phenylene groups released the ibuprofen molecules much more slowly compared to the corresponding samples functionalized with bridging ethane and ethylene groups as well as unfunctionalized MCM-41 material (Fig. 7C). This is more likely due to the fact that the sample containing phenyl groups forms favorable π–π interaction with the ibuprofen molecule, limiting its release into the solution.

These differences in adsorption and release properties among the samples for R6G and ibuprofen molecules are promising because they show how rational synthesis and functionalization of mesoporous materials create nanomaterials with high adsorption capacity and controlled drug release properties. By further functionalization of the materials with other bioactive functional groups such as antibodies and PNAs on the external surfaces of the materials, the targeting of specific sites in the body by these materials could also be possible in addition to the controlled release of large cargo of drug molecules.

4 Conclusions

We have demonstrated the synthesis of various monofunctionalized and multifunctionalized mesoporous materials that have different and enhanced drug adsorption capacity and drug release properties. The synthesis of the materials was achieved by one pot co-condensation or by grafting synthetic methods. By the incorporation of different functional groups, the adsorption and drug release properties of rhodamine 6G and ibuprofen from the materials were changed. By taking advantage of the different adsorption and release properties based on the careful choice of functional groups, it will be possible to obtain nanomaterial drug delivery vehicles with optimized adsorption and controlled release properties.

Acknowledgements We gratefully acknowledge the financial assistance by the US National Science Foundation (NSF), CAREER Grant No. CHE-064534, for this work. E.A.B. and A.N.O. were partially supported in 2006 and 2007, respectively, by NSF–REU, Grant No. CHE-0552753, which was awarded to Chemistry Department at Syracuse University.

References

Anan, A., Sharma, K.K., Asefa, T.: J. Mol. Catal. A. **288**, 1 (2008)
Asefa, T., MacLachlan, M.J., Coombs, N., Ozin, G.A.: Nature **402**, 867 (1999)
Balas, F., Manzano, M., Horcajada, P., Vallet-Regí, M.: J. Am. Chem. Soc. **128**, 8116 (2006)
Beck, J.S., Vartuli, J.C., Roth, W.J., Leonowicz, M.E., Kresge, C.T., Schmitt, K.D., Chu, C.T.W., Olson, D.H., Sheppard, E.W., McCullen, S.B., Higgins, J.B., Schlenker, J.L.: J. Am. Chem. Soc. **114**, 834 (1992)
Cheng, C.F., Luan, Z.H., Klinowski, J.: Langmuir **11**, 2815 (1995)
Corriu, R., Mehdi, A., Reye, C.: J. Organometallic Chem. **689**, 4437 (2004)
Doadrio, J.C., Sousa, E.M.B., Izquierdo-Barba, I., Doadrio, A.L., Pérez-Pariente, J., Vallet-Regí, M.: J. Mater. Chem. **16**, 462 (2006)
Dong, W.Y., Sun, Y., Lee, C.W., Hua, W., Lu, X., Shi, Y., Zhang, S., Chen, J., Zhao, D.: J. Am. Chem. Soc. **29**, 13894 (2007)
Fryxell, G.E., Liu, J., Hauser, T.A., Nie, Z., Ferris, K.F., Mattigod, S., Meiling, G., Hallen, R.T.: Chem. Mater. **11**, 2148 (1999)
Gadre, S.Y., Gouma, P.I.: J. Am. Cer. Soc. **89**, 2987 (2006)
Giri, S., Trewyn, B.G., Lin, V.S.-Y.: Nanomedicine **2**, 99 (2007)
Gu, J., Fan, W., Shimojima, A., Okubo, T.: Small **3**, 1740 (2007)
Hicks, J.C., Dabestani, R., Buchanan, A.C., Jones, C.W.: Chem. Mater. **18**, 5022 (2006)
Holland, B.T., Blanford, C.F., Stein, A.: Chem. Mater. **11**, 3302 (1999)
Horcajada, P., Rámila, A., Ferey, G., Vallet-Regí, M.: Solid State Sci. **8**, 1243 (2006)
Huang, S., Yang, P., Cheng, Z., Li, C., Fan, Y., Kong, D., Lin, J.: J. Phys. Chem. C **112**, 7130 (2008)
Huo, Q., Margolese, D.I., Stucky, G.D.: Chem. Mater. **8**, 1147 (1996)
Inagaki, S., Fukushima, Y., Kuroda, K.: J. Chem. Soc., Chem. Commun. 680 (1993)
Inagaki, S., Guan, S., Fukushima, Y., Ohsuna, T., Terasaki, O.: J. Am. Chem. Soc. **121**, 9611 (1999)
Kim, H.-J., Ahn, J.-E., Haam, S., Shul, Y.-G., Song, S.-Y., Tatsumi, T.: J. Mater. Chem. **16**, 1617 (2006)
Kokubo, T., Kushitani, H., Sakka, S., Kitsugi, T., Yamamuro, T.: J. Biomed. Mater. Res. **24**, 721 (1990)
Kresge, C.T., Leonowicz, M.E., Roth, W.J., Vartuli, J.C., Beck, J.S.: Nature **359**, 710 (1992)
Kruk, M., Asefa, T., Jaroniec, M., Ozin, G.A.: Stud. Surf. Sci. Catal. **141**, 197 (2002)
Lai, C.Y., Trewyn, B.G., Jeftinija, D.M., Jeftinija, K., Xu, S., Jeftinija, S., Lin, V.S.-Y.: J. Am. Chem. Soc. **125**, 4451 (2003)
Law, M., Greene, L.E., Johnson, J.C., Saykally, R., Yang, P.: Nat. Mater. **4**, 455 (2005)
Lim, M.H., Blanford, C.F., Stein, A.: J. Am. Chem. Soc. **119**, 4090 (1997)
Mal, N.K., Fujiwara, M., Tanaka, Y.: Nature **421**, 350 (2003)
Margolese, D., Melero, J.A., Christiansen, S.C., Chmelka, B.F., Stucky, G.D.: Chem. Mater. **12**, 2448 (2000)
Moller, K., Bein, T.: Chem. Mater. **10**, 2950 (1998)
Muñoz, B., Rámila, A., Díaz, I., Pérez-Pariente, J., Vallet-Regí, M.: Chem. Mater. **15**, 500 (2003)
Patel, K., Angelos, S., Dichtel, W.R., Coskun, A., Yang, Y.-W., Zink, J.I., Stoddart, J.F.: J. Am. Chem. Soc. **130**, 2382 (2008)
Qu, F., Zhu, G., Lin, H., Sun, J., Zhang, D., Li, S., Qiu, S.: Eur. J. Inorg. Chem. 3943 (2006)
Radu, D.R., Lai, C.-Y., Wiench, J.W., Pruski, M., Lin, V.S.-Y.: J. Am. Chem. Soc. **126**, 1640 (2004)
Sayari, A., Hamoudi, S.: Chem. Mater. **13**, 3151 (2001)
Sharma, K.K., Asefa, T.: Angew. Chem., Int. Ed. **46**, 2879 (2007)
Sharma, K.K., Anan, A., Buckley, R.P., Ouellette, W., Asefa, T.: J. Am. Chem. Soc. **130**, 218 (2008)

Song, S.-W., Hidajat, K., Kawi, S.: Langmuir **21**, 9568 (2005)
Stein, A., Melde, B.J., Schroden, R.C.: Adv. Mater. **12**, 1403 (2000)
Suh, M., Lee, H.-J., Park, J.-Y., Lee, U.-H., Kwon, Y.-U., Kim, D.J.: Chem. Phys. Chem. **9**, 1402 (2008)
Tang, Q.-L., Xu, Y., Wu, D., Sun, Y.-H., Wang, J., Xu, J., Deng, F.: J. Control. Release **114**, 41–46 (2006)
Thomas, J.M., Raja, R.: Chem. Record **1**, 448 (2001)
Vallet-Regi, M.: Chem. Eur. J. **12**, 5934 (2006)
Vallet-Regi, M., Balas, F., Arcos, D.: Angew. Chem., Int. Ed. **46**, 7548 (2007)
Walcarius, A., Etienne, M., Lebeau, B.: Chem. Mater. **15**, 2161 (2003)
Whitesides, G.M.: Small **1**, 172 (2005)
Wu, Z., Joo, H., Ahn, I.-S., Kim, J.-H., Kim, C.-K., Lee, K.: J. Non-Cryst. Solids **342**, 46 (2004)
Yanagisawa, T., Shimizu, T., Kuroda, K., Kato, C.: Bull. Chem. Soc. Jpn. **63**, 1535 (1990)
Yang, P., Huang, S., Kong, D., Lin, J., Fu, H.: Inorg. Chem. **46**, 3203 (2007a)
Yang, P., Quan, Z., Lu, L., Huang, S., Lin, J., Fu, H.: Nanotechnology **18**, 235703 (2007b)
Yang, P., Lu, L., Quan, Z., Huang, S., Lin, J.: Biomaterials **29**, 692 (2008)
Zapilk, C., Liang, Y., Nerdal, W., Anwander, R.: Chem. Eur. J. **13**, 3169 (2007)
Zeng, W., Qian, X.-F., Yin, J., Zhu, Z.-K.: Mater. Chem. Phys. **97**, 437 (2006)
Zhu, Y.F., Shi, J.-L., Li, Y.-S., Chen, H.-R., Shen, W.-H., Dong, X.-P.: J. Mater. Res. **20**, 54 (2005)